Hindawi Publishing Corporation
International Journal of Aerospace Engineering
Volume 2015, Article ID 694564, 9 pages
http://dx.doi.org/10.1155/2015/694564

Research Article

Modeling of the Diffusion Bond for SPF/DB Titanium Hollow Structures

Xianghai Chai,[1] Xiaoyun Zhang,[2] Zhiqiang Wang,[1] and Yesheng Liu[1]

[1]*China Aerospace Research Institute of Shanghai Branch, AVIC Commercial Aircraft Engine Co., Ltd., Shanghai 201108, China*
[2]*Department of Mechanical Engineering, Shanghai Jiao Tong University, Shanghai 201108, China*

Correspondence should be addressed to Zhiqiang Wang; wangzq@acae.com.cn

Received 5 September 2014; Accepted 29 December 2014

Academic Editor: Debes Bhattacharyya

Diffusion-bonded titanium hollow warren structures have been successfully applied in aircraft engine components, such as fan blade, and OGV, while the optimal design of the hollow warren structure to improve its impact resistance, especially under bird-strike event, has been a challenge. In this work, a series of impact tests and numerical simulations are carried out to investigate the effect of key geometric features on the overall impact strength of a panel-shaped titanium hollow warren structure. Based on experimental and numerical studies, a quantitative relationship between diffusion bonding seam strength and the overall impact strength is developed. Meanwhile, key geometric factors affecting the resultant bonding seam strength for a typical manufacturing process are identified. This work provides useful references for the optimal design to increase impact resistance for aircraft engine hollow warren structure components.

1. Introduction

Driven by the development of high bypass ratio turbo-fan engine, titanium hollow components with internal Warren girder structure have been widely used to meet the weight reduction requirement of the engine. In 1980's, a wide-chord titanium hollow fan blade with Warren girder structure was developed by Rolls-Royce using the diffusion bonding/superplastic forming (SPF/DB) process [1, 2]. The application of Warren girder hollow structure can lead to 10%~30% weight saving on the rotor. In addition, the hollow structure allows the designer to optimize the overall strength of the component by merely tuning its internal configuration, while the external geometry is fixed to keep the aero performance of the component unchanged. For hollow fan blade, optimizing the internal structure to improve the bird-strike performance of the blade has been a continuous effort of the industry [3].

Debonding at the diffusion welding interfaces is one of the major failure modes of the Warren girder hollow structures under impact loads, and the strength of the diffusion bond significantly influences the overall impact resistance of the hollow blade. Ideally, the strength of the diffusion bond should be close to the parent material, while, in practical engineering applications, the welding interface is often a weak point for multiple reasons [4–6]. First, it is very difficult to guarantee a 100% bonding rate at welding interface in the actual DB/SPF process, and, for a given process, the local bonding defect distribution may vary from place to place although the overall bonding rate is still within the spec limit of the product. On the other hand, dependent on the local geometry of Warren girder structure, stress concentration may occur at the edge of the welding interface, and, consequently, lead to the reduction of failure threshold of the bond [7]. Therefore, the overall failure strength of the Warren girder structure is the result of a combined effect of manufacturing process and geometric features.

Direct experimental measurement of the strength of the bonding interface is costly since the strength value may vary at different locations. Beside, to accurately capture the stress concentration at the edge of the bonding interface, very fine mesh is needed at these locations for the numerical model, which will involve high computational cost. For a practical bird-strike analysis model for the hollow fan blade, the stress concentration at the edge of the bonding interface is usually underestimated due to the coarse mesh. For the above reasons, a feasible approach to consider the bond effect is to

introduce phenomenological *effective failure strength* of the bond in the analytical model, which reflects the effects of both bonding interface defects and local stress concentration. The effective failure strength of the bond needs to be determined through inverse method based on impact tests.

For simplification, it is assumed that the defect distribution is merely a function of geometric characteristics. This assumption is reasonable for a specific Warren girder hollow component manufactured with a relatively matured SPF/DB process, since the deviation of process parameters (e.g., temperature, pressure, and surface quality) is mainly determined by the location and local geometric features in this case. On the other hand, the stress concentration is also dependent on local geometric parameters. Therefore, it is possible to establish a relatively simple mapping between the major geometric parameters of the Warren girder structure and the resultant impact strength, which can provide useful reference for the designers.

In this study, a set of ballistic impact tests with titanium hollow panels with various internal geometric parameters were conducted to explore the effect of major geometric characteristics on the impact strength. The panel-shape specimens were designed to simulate a typical Warren girder configuration used in hollow fan blade. An inverse method based on the correlation of test and numerical simulation was used to estimate the effective failure strength of the diffusion bonds for different Warren girder structures. Based on the above experimental and analytical results, a qualitative relation between the failure stresses of the diffusion bonds and two important geometric parameters, skew angle of the girder, and length of the diffusion bond was established. This study provided a useful reference for the optimal design of components with Warren girder hollow structures. Furthermore, a hollow fan blade model was developed to demonstrate the implementation of the effective bond strength based on its internal structure features and was then used to show the effect of the debonding of the diffusion bond on the overall impact resistance of the hollow fan blade under bird-strike.

2. The SPF/DB Warren Girder Structure

The typical geometry of the Warren Girder structure formed with SPF/DB process is shown in Figure 1. The structure consists of two face sheets and one core sheet. The face sheets and the core sheet are connected through diffusion bond along the prescribed welding lines. The trapezoidal girder structure is formed through a super-plastic forming process, in which the sheets are stretched and distorted under the inert gas injection between the gaps of the sheets, as shown in Figure 2.

The impact strength of the warren girder hollow structure is largely dependent on the strength of the diffusion bonds, while the latter is related to the geometric features of the hollow structure itself. In order to investigate the relation between the impact strength and the geometrical features, the size of the diffusion bond and the geometric profile of the girder must be taken into account. The key parameters in this paper are defined as follows (Figure 1) [8]:

(1) the thickness of the face sheet $T1$;

(2) the thickness of the original core sheet $T2$;

(3) the thickness of the core sheet after super-plastic forming process $T3$;

(4) the skew angle of the girder α;

(5) the length of a hollow region bond D, the length of leading edge bond D_1, and the length of trailing edge bond D_2 ($D_1 = D_2$).

In this study, a set of titanium Warren girder hollow flat panels with straight welding lines has been used as test specimens to investigate the effect of geometric characteristics on the impact strength. The flat panels are shown in Figure 3. The geometric parameters of the girder were selected within the practical range for the actual SPF/DB process.

3. Hollow Panel Impact Test and Analysis

3.1. High Speed Impact Test for the Hollow Panel. In this work, a series of hollow panel impact tests were conducted to investigate the failure mechanisms of the panel under high speed impact loads. Each test piece has a dimension of 290 mm in length by 130 mm in width. The test equipment consists of a high speed gas gun of 150 mm caliber. The panels were shot to impact the target plate made of aluminum, which is a common candidate material for fan case, in the vertical direction. Three sets of hollow panel with different hollow structure parameters were tested. The impact velocities are chosen to be 160 m/s, 175 m/s, and 190 m/s, respectively. An example of the test pieces after impact is shown in Figure 4. It shows that the panel was torn apart along the diffusion bonding interfaces under the impact load, with both face-sheets curling backward.

The test results are listed in Table 1, illustrating the impact velocity and the impact energy. The correlation between the structural parameters of the hollow panels and the diffusion bond failure stresses will be analyzed.

3.2. Inverse Analysis for the Bond Strength Estimation. The focus of this study is to estimate the failure stress of the diffusion bonds of the titanium Warren girder hollow structure. Due to the complexity of the structure, the bond strength is difficult to be directly measured. Therefore, an inverse analysis is performed to estimate the bond strength. In the inverse method, finite element simulation models are built with assumed bond failure stresses, which vary in the reasonable range, and then an optimization algorithm is used to find the values of the tensile and shear failure stresses of the bond corresponding to the minimum of a predefined object function, which describes the averaged prediction error of the deformation and failure of the simulation model compared with test results. Such values are considered as the effective tensile and shear failure stresses, respectively, of the diffusion bond corresponding to different hollow structures.

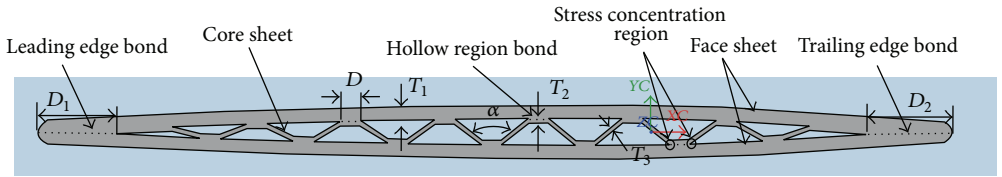

Figure 1: Geometric parameters of hollow structure.

Table 1: Results of hollow panel impact tests.

Test number	Girder skew angle (°)	Leading/trailing edge bond length (mm)	Hollow region bond (mm)	core sheet/face-sheet thickness (mm)	Panel weight (Kg)	Impact velocity (m/s)	Impact energy ($\times 10^3$ J)
Number 1	30	10	2	0.5/2	0.726	213	16.47
Number 2	45	13	2	0.5/1.5	0.586	163	7.78
Number 3	45	8	2	0.5/1.5	0.544	214	12.46

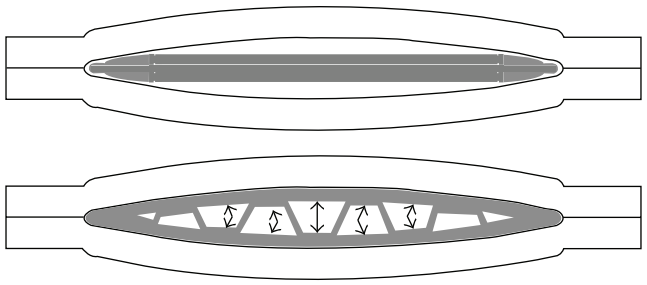

Figure 2: The superplastic forming method based air pressure.

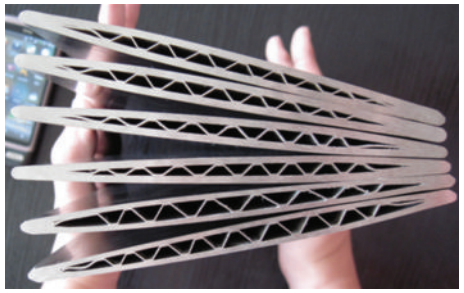

Figure 3: The titanium Warren girder hollow panel used as test specimen.

The simulation of the hollow panel impact tests were conducted with the explicit commercial finite element code LS-DYNA. Due to the high strain rate during the impact, the materials hardening behavior with strain rate dependency must be taken into account. In the finite element model, a tie-break contact algorithm is adopted to simulate the welding and interface and predict the debonding failure. The finite element model used in this study is shown in Figure 5. Single integration point solid elements are used all over the model, and the mesh size at the girders is set to around 2 mm. This mesh profile is selected after a number of test runs and can provide enough fidelity to capture the deformation and failure of the girder with reasonable computational cost.

3.2.1. The Inverse Method. An appropriate optimization model and algorithm are essential for the effectiveness of the inverse analysis. Traditional optimization methods include the simple linear programming and various iterative gradient algorithms based on the nonlinear programming (e.g., the steepest descent method and the conjugate gradient method) [9].

The sequential quadratic programming (SQP) method has been employed in this study [10]. The girder skew angle, bond length, and the core sheet/face-sheet thickness are selected as the primary influential factors on failure characteristic of the specimen, while the strength of the bond has to be determined for different hollow structures.

Apart from the above factors, the influence of other unknown preimpact parameters, such as the welding line curvature and material defects, are estimated from engineering experiences. Some postimpact parameters, for example, the deformation and failure mechanisms, are used as constraint conditions. The complete inverse analysis procedure is implemented by coupling the commercial codes LS-DYNA and OPTIMUS, with the principal aspects explained in details below.

(1) Optimization Objective Function Based on the Deformation of the Hollow Panel. With the tensile and shear failure stresses as the input variables, the deformation of the impacted hollow panel is used to construct the objective function to be optimized. Mathematically, the optimization problem can be expressed as [11]

$$F(x) = \sum_k \omega_k \left(\frac{y_k - y_{\text{obj}}}{y_{\text{obj}}} \right)^2, \quad k = 1, 2, \ldots, m, \tag{1}$$

$$y_k = f(x_1, x_2 \cdots x_n), \tag{2}$$

$$g_i(x) \le c_i, \quad i = 1, 2, \ldots, n, \tag{3}$$

$$s_i^{l(m)} \le x_i \le s_i^{u(m)}, \quad i = 1, 2, \ldots, p, \tag{4}$$

where (1) represents the scalar objective function formulated as a weighted sum of the square of the relative error. Equation

Figure 4: Deformed hollow panel after impact.

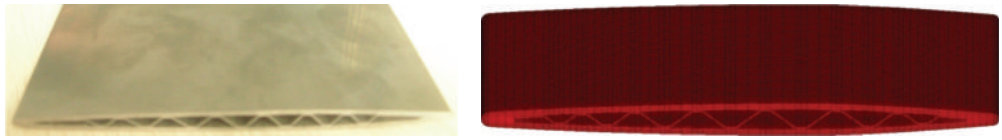

Figure 5: Finite element model of the hollow panel.

(2) describes the relationship between the input variables and the hollow panel deformation amount in numerical simulation. By manual analysis, the influence of input variables, such as the material model, the mesh density, and contact stiffness, for simulation results can be determined. And only the tensile failure stress and shear failure stress of the bond are retained as input variables in the inverse analysis. Equations (3) are the constraints imposed on the input variables, and (4) give the design range of the variables. Among them, y_{obj} is the target value of the hollow panel deformation given by impact test results, and y_k is the calculated result at each optimization iteration. Here, ω_k is the weighting coefficient, and $s_i^{l(m)}$ and $s_i^{u(m)}$ denote the lower and upper bounds of the input variables based on empirical knowledge. When the tensile failure stress and shear failure stress of weld are set as input parameters, y_{obj} changes with the bond strength.

(2) Bond Failure Constraints. In the inverse analysis, the objective function is defined as the deformation of the panel, which is determined by the displacement values at a certain group of nodes. However, the whole impact process cannot be described merely by nodal displacement, and the failure progress of the bond area needs to be considered as well. Thus, the bond failure prediction in noncontacted area is employed as a supplementary constraint to yield more precise reconstruction of impact process.

3.2.2. Inverse Analysis Procedures. As shown in Table 2, the tensile and shears stresses of the bond (denoted as σ_{1i}, τ_{1i}, σ_{2i}, τ_{2i} and σ_{3i}, τ_{3i} for different tests, resp.) are set as input variables with the reasonable ranges estimated based on the titanium welding interface strength obtained by simple performance tests.

The objective function is defined as the summation of deformation amounts at three locations on the hollow panel. The three locations are within the hollow Warren girder region and the solid regions at the leading/trailing edges, respectively, as shown in Table 3. Considering the effect of other structural factors on the panel deformation, different weighting factors are applied for different location of consideration. Thus (1) is rewritten as follows:

$$
\begin{aligned}
F(x) &= \left(0.2 * (\$\text{Opt1}\$)^2 + 0.4 * (\$\text{Opt2}\$)^2 \right. \\
&\quad \left. +0.4 * (\$\text{Opt3}\$)^2\right)^{0.5} \\
\$\text{Opt1}\$ &= \frac{(\$D1\$ - (\$\text{Pos}x11\$ - \$\text{Pos}x12\$))}{(\$\text{Pos}x11\$ - \$\text{Pos}x12\$)} \\
\$\text{Opt2}\$ &= \frac{(\$D2\$ - (\$\text{Pos}x21\$ - \$\text{Pos}x22\$))}{(\$\text{Pos}x21\$ - \$\text{Pos}x22\$)} \\
\$\text{Opt3}\$ &= \frac{(\$D3\$ - (\$\text{Pos}x31\$ - \$\text{Pos}x32\$))}{(\$\text{Pos}x31\$ - \$\text{Pos}x32\$)},
\end{aligned}
\tag{5}
$$

where $F(x)$ is the objective function, \$Opt$k$\$ (k = 1~3) represents the relative error of the titanium hollow panel deformation at the measuring point, and \$$Dk$\$ is the test result of the panel deformation. \$Posxk1\$ and \$Posxk2\$ denote the coordinates of a certain node on upper face-sheet and the lower face-sheet, respectively. Then, (\$Posxk2\$ – \$Posxk1\$) is the analytical result of the panel deformation at various locations.

The constraints of the optimization problem are imposed such that the deformation (relative nodal displacement between upper and lower face-sheets) in noncontact area must lie within the given limit. The nodes with the maximum magnitude of deformation are chosen for evaluation. The constraint parameters are shown in Table 3.

3.2.3. Inverse Analysis Results. The performance of optimization procedure can be illustrated by taking the test number 1 in Table 1, for instance. The Latin hypercube designs

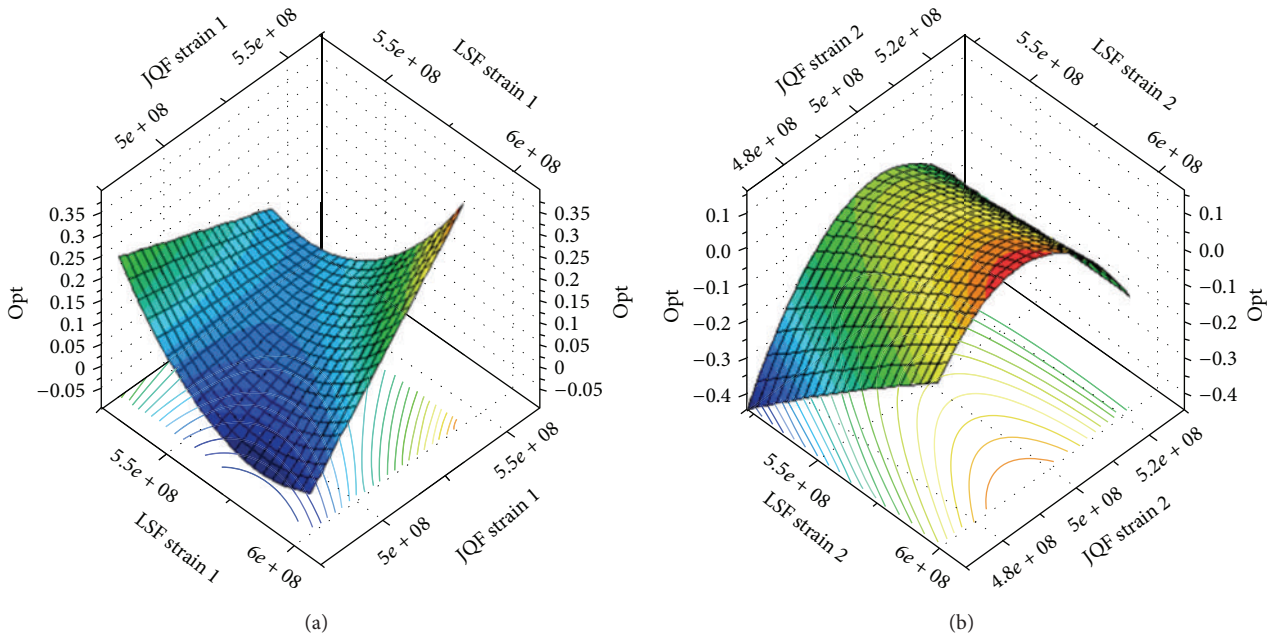

Figure 6: Response surface models for objective function.

Table 2: Input variables and value range.

x_i	Input variable	Diffusion bond position	Initial value	Lower boundary	Lower boundary
Number 1 (σ_{1i}/τ_{1i})	The tensile and shears stress for number 1 (Pa)	Hollow region	$5.10E+8/4.55E+8$	$4.80E+8/4.25E+8$	$5.40E+8/4.85E+8$
		Leading/trailing edge	$5.25E+8/4.75E+8$	$4.95E+8/4.45E+8$	$5.55E+8/4.95E+8$
Number 2 (σ_{2i}/τ_{2i})	The tensile and shears stress for number 2 (Pa)	Hollow region	$5.35E+8/4.85E+8$	$5.05E+8/4.55E+8$	$5.65E+8/5.15E+8$
		Leading/trailing edge	$5.45E+8/4.95E+8$	$5.25E+8/4.75E+8$	$5.55E+8/5.25E+8$
Number 3 (σ_{3i}/τ_3)	The tensile and shears stress for number 3 (Pa)	Hollow region	$5.60E+8/5.15E+8$	$5.30E+8/4.85E+8$	$5.90E+8/5.45E+8$
		Leading/trailing edge	$5.75E+8/5.35E+8$	$5.45E+8/4.95E+8$	$5.95E+8/5.55E+8$

Table 3: Constraint parameters.

y_i	Optimization and constraints parameters	Object value
D_1	The deformation at 9 mm to the impact edge	2.5 mm
D_2	The deformation at 17 mm to the impact edge	3 mm
D_3	The deformation at 27.5 mm to the impact edge	1.75 mm
D_d	The deformation at 50 mm to the impact edge	0 mm

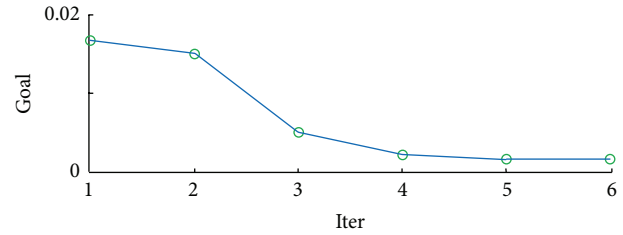

Figure 7: Optimization convergence curve.

(LHDs) are firstly employed to evaluate the correlation values between the input variables, resulting in the objective function values, of which the response surface model (RSM) is then generated by fitting the experimental data using the Least Squares Fitting [12].

The response surface model of the objective function (Opt) in terms of the input variables (σ_1, τ_1) is shown in Figure 6(a). It shows that the range of σ_{11} and τ_{11} at the hollow Warren girder region can be redefined as $(5.50E+8, 5.85E+8)$ and $(4.85E+8, 5.10E+8)$, respectively. Similarly, the range of σ_{12} and τ_{12} at the leading/trailing edge (Figure 6(b)) can be redefined as $(5.75E+8, 5.90E+8)$ and $(5.00E+8, 5.20E+8)$, respectively, to narrow the searching scope of optimization and speed up the convergence.

Based on the RSM results, σ_{11}, τ_{11}, σ_{12}, and τ_{12} take central values of $5.68E+8$ Pa, $4.98E+8$ Pa, $5.83E+8$ Pa, and $5.10E+8$ Pa, respectively, which are set as the respective initial values of the optimization. The sequential quadratic programming method is used as the optimization algorithm. As shown in Figure 7, the optimization converges to [$5.60E+8$ Pa, $5.10E+8$ Pa, $5.59E+8$ Pa, $5.09E+8$ Pa] after 6 iterations.

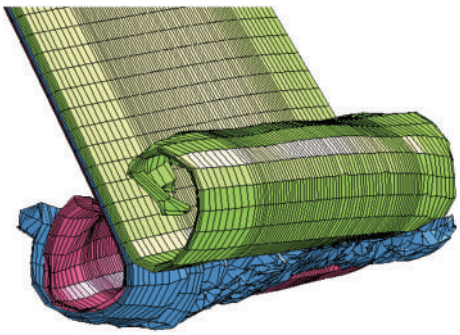

Figure 8: Simulation result at optimized point.

The corresponding result of deformation of the titanium hollow panel is shown in Figure 8.

3.3. Correlation between Geometrical Features and Impact Resistance. Using the same approach, the bond strength of tests number 2 and number 3 can be obtained. Through the correlation analysis, it was found that the face-sheet thickness has little effect on the bond strength. Thus only the effect of the girder skew angle and the bond length will be considered.

For the three sets of hollow panels listed in Table 1, specimens number 2 and number 3 have the same girder skew angle, while the bond length is 8 mm and 13 mm, respectively. Due to the limited sample size, a linear relation between the bond length and the bond strength is assumed. Therefore, the bond strength for a panel with the bond length of 10 mm and skew angle of 45 degree can be interpolated from the results of tests number 2 and number 3. From the calculated results for the three sets of panel tests, the effect of the skew angle and the bond length can be estimated, as shown in Table 4.

The analysis shows that the bond length and girder skew angle of titanium Warren girder structures are the two sensitive factors affecting the bond strength within the range of the test piece's design parameters and need to be carefully chosen in the hollow component design. Based on this study, increasing the bond length and decreasing skew angle within the feasible range are recommended in the hollow component design.

With the above estimation of the diffusion bond strength for various geometric features, the tensile and shear failure stresses of a specific hollow fan blade design can easily be given based on the local internal geometric characteristics. Such failure stress values can then be used in the simulation models for the prediction of the bird-strike performance of the fan blade design.

4. Hollow Fan Blade Bird-Strike Analysis

The sensitivity of the geometric parameters of the hollow structure on the bond strength has been shown in the previous section. The implementation of the effective bond strengths based on the internal structure features in a hollow fan blade bird-strike model will be discussed in this section. The hollow fan blade to be modeled is a SPF/DB hollow blade with a Warren girder internal structure. The typical cross section of the blade near the midspan is shown in Figure 9. The blade has a uniform skew angle of 45 degrees. The thickness of the core sheet is 2 mm. The hollow region bond lengths are 2 mm at the girder areas in the middle. The bond length at the leading edge varies from 7 mm to 9 mm along the span direction, with an average of 8 mm, while the bond length at the trailing edge varies from 12 mm to 14 mm, with an average of 13 mm.

Figure 9: The cross section of the hollow fan blade to be modeled.

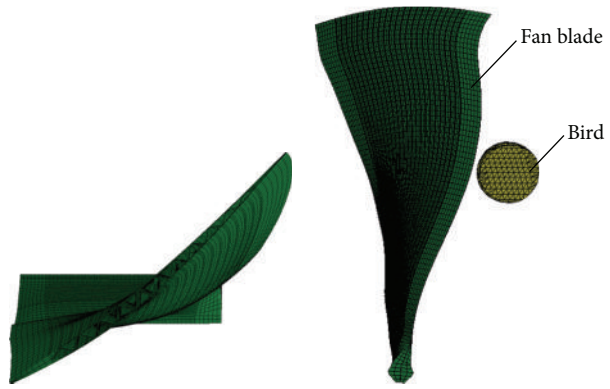

Figure 10: The bird-strike model for hollow fan blade.

4.1. The Bird-Strike Simulation. The bird-strike analysis model for this fan blade is shown in Figure 10. Tie-break contacts are incorporated at the diffusion bonding areas, where the effective tensile and shear strengths are estimated from Table 4. It is noted that, unlike the hollow flat panel in the tests, the geometry of the blade is not symmetric anymore, and the cross section is not constant along the span direction, either. For simplification, the averaged bond length is used to estimate the effective bond strengths for both the leading edge and the trailing edge. And for the hollow region, the value of bond strength is chosen as that corresponding to the edge bond length of 10 mm, which is simply the rough value of the averaged bond length for both edges. The values of the bond strengths are listed in Table 5.

The bird impact is simulated through ALE (arbitrary Lagrangian-Eulerian) algorithm, where the bird is model with Euler algorithm. The bird weights 3 lbs. The impact location is set to the 60% span. The rotational speed of the blade is 3000 rpm.

The simulation result is shown in Figure 11. Material loss is observed near the impact area, and significant debonding occurs around this area. There is an obvious peak spot of the plastic strain near the blade root on the leading edge. Such damage profile is often seen in typical blade bird-strike tests.

4.2. The Effect of Debonding of the Diffusion Bonds. To show the effect of debonding of the diffusion bonds on the blade

Table 4: The relation between structure parameters and bond strength.

	Parameters	Hollow region tensile failure stress (Pa)	Hollow region shear failure stress (Pa)	Leading/trailing edge tensile failure stress (Pa)	Leading/trailing edge shear failure stress (Pa)
Girder skew angle	30° (10 mm)	$5.60E+8$	$5.10E+8$	$5.89E+8$	$5.33E+8$
	45° (10 mm)	$5.23E+8$	$4.58E+8$	$5.59E+8$	$4.90E+8$
Leading/trailing edge bond length	8 mm (45°)	$5.13E+8$	$4.52E+8$	$5.49E+8$	$4.83E+8$
	13 mm (45°)	$5.37E+8$	$4.67E+8$	$5.74E+8$	$5.00E+8$

Table 5: The bond strength parameters.

	Failure parameters	Parameters value
σ_c	Tensile failure stress at hollow region	$5.23E+8$ Pa
τ_c	Shear failure stress at hollow region	$4.58E+8$ Pa
σ_{le}	Tensile failure stress at leading edge	$5.74E+8$ Pa
τ_{le}	Shear failure stress at leading edge	$5.00E+8$ Pa
σ_{te}	Tensile failure stress at trailing edge	$5.49E+8$ Pa
τ_{te}	Shear failure stress at trailing edge	$4.83E+8$ Pa

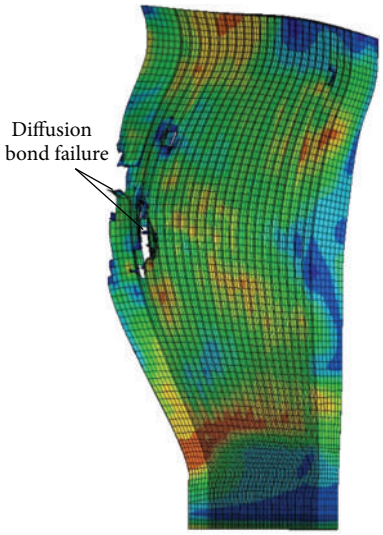

Figure 11: The blade deformation and failure.

damage under impact, a separated model without simulating diffusion bonds is developed and compared with the one with diffusion bonding. Same mesh profile is used in both models. Figure 12 shows the plastic strain contour at the blade root for both models. It is found that the model without diffusion bonds gives nearly 20% higher plastic strain, as shown in Figure 13, at the root area. This is reasonable since more kinetic energy is absorbed through debonding for the model with diffusion bonds simulated. The model without modeling diffusion bonding obviously overpredicted the blade damage. This example shows the necessity of the appropriate simulation of the diffusion bond in the bird-strike analysis for the hollow blade.

5. Conclusion

The geometric features of titanium hollow structure are found to have considerable effects on the impact resistance of hollow structure. In this study, a number of geometric factors are investigated and a qualitative relationship between these factors and the strength of the diffusion bond under impact load was established through a series of impact tests combined with numerical simulations. The tensile and shear failure stresses of the diffusion bond for various Warren girder titanium hollow panels were estimated through an inverse method.

The analysis shows that the bond strength is significantly dependent on the bond length and girder skew angle. These two parameters need to be carefully chosen in the hollow component design. Based on this study, increasing the bond length and decreasing skew angle within the feasible range are recommended in the hollow component design.

A hollow fan blade model was developed to demonstrate the implementation of the effective bond strength based on its internal structure features. From the comparison between the result of this model and that of the model without diffusion bond simulated, it can be observed that the effect of the debonding of the diffusion bond on the blade damage is significant. This means appropriate modeling of the diffusion bond is important in impact analysis of the hollow fan blade.

Although the proposed method can provide a quick approach to estimate the impact performance of the particular hollow component design, it should be noted that the effect of some important factors was estimated through engineering experience because of the limit on computational and experimental cost. For example, processing parameters and defect effects are not modeled explicitly. Also, the larger sample size and the geometric parameter range in the test needs to be considered in our future study.

Nomenclature

$T1$: Thickness of the face sheet, (mm)
$T2$: Thickness of the original core sheet, (mm)
$T3$: Thickness of the core sheet after super-plastic forming process, (mm)
α: Skew angle of the girder
D: Length of a single diffusion bond, (mm)
D_1: The length of leading edge bond, (mm)
D_2: The length of trailing edge bond, (mm)
σ_c: Tensile failure stress at cavity position, (Pa)

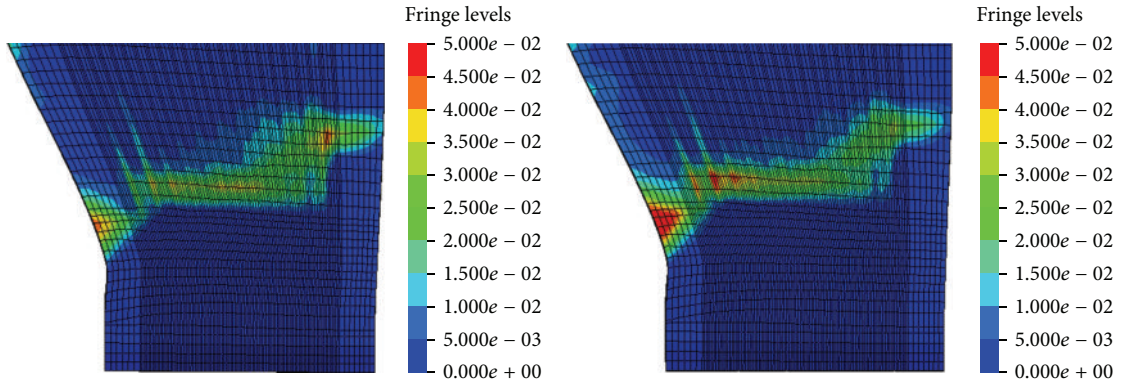

(a) Model diffusion bonds simulated (b) Model nondiffusion bonds simulated

FIGURE 12: Contour plots of effective plastic strain near blade root.

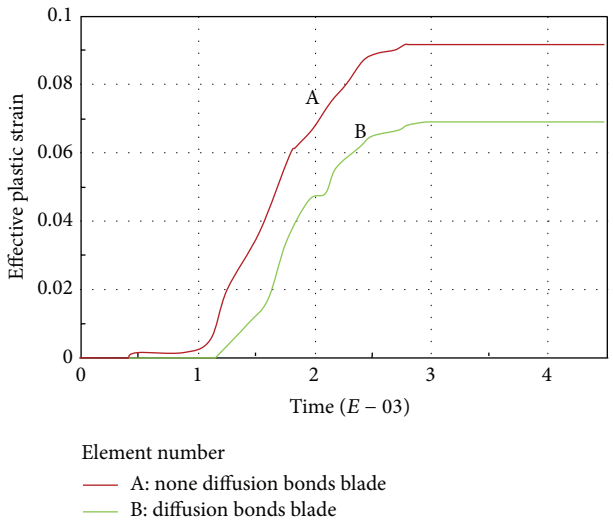

FIGURE 13: Comparison of effective plastic strain near blade root.

τ_c: Shear failure stress at cavity position, (Pa)
σ_{le}: Tensile failure stress at leading edge, (Pa)
τ_{le}: Shear failure stress at leading edge, (Pa)
σ_{te}: Tensile failure stress at trailing edge, (Pa)
τ_{te}: Shear failure stress at trailing edge, (Pa).

Abbreviations

SPF/DB: Super-plastic forming/diffusion bonding
SQP: Sequential quadratic programming
LHDs: Latin Hypercube Designs
RSM: Response Surface Model
ALE: Arbitrary Lagrangian-Eulerian.

Conflict of Interests

The authors declare that there is no conflict of interests regarding the publication of this paper.

Acknowledgments

The authors gratefully acknowledge the support from The National Natural Science Foundation of China (No. 51205377), The Foundation of Science and Technology Commission of Shanghai (No. 12DJ1400500), and Aeronautical Science Foundation of China (No. 2012ZBN2003).

References

[1] J. Bonet, A. Gil, R. D. Wood, R. Said, and R. V. Curtis, "Simulating superplastic forming," *Computer Methods in Applied Mechanics and Engineering*, vol. 195, no. 48-49, pp. 6580–6603, 2006.

[2] S. Audic, M. Berthillier, J. Bonini et al., "Prediction of bird strike in Hollow Fan Blades," in *Proceedings of the 36th AIAA/ASME/SAE/ASEE Joint Propulsion Conference and Exhibit*, Huntsville, Ala, USA, July 2000.

[3] G. Y. Li, M. J. Tan, and K. M. Liew, "Three-dimensional modeling and simulation of superplastic forming," *Journal of Materials Processing Technology*, vol. 150, no. 1-2, pp. 76–83, 2004.

[4] Y. Chen, K. Kibble, R. Hall, and X. Huang, "Numerical analysis of superplastic blow forming of Ti-6Al-4V alloys," *Materials and Design*, vol. 22, no. 8, pp. 679–685, 2001.

[5] K. Deb, A. Pratap, S. Agarwal, and T. Meyarivan, "A fast and elitist multiobjective genetic algorithm: NSGA-II," *IEEE Transactions on Evolutionary Computation*, vol. 6, no. 2, pp. 182–197, 2002.

[6] S.-Y. Chen, "An approach for impact structure optimization using the robust genetic algorithm," *Finite Elements in Analysis and Design*, vol. 37, no. 5, pp. 431–446, 2001.

[7] H. Kurtaran, A. Eskandarian, D. Marzougui, and N. E. Bedewi, "Crashworthiness design optimization using successive response surface approximations," *Computational Mechanics*, vol. 29, no. 4-5, pp. 409–421, 2002.

[8] J. Forsberg and L. Nilsson, "Evaluation of response surface methodologies used in crashworthiness optimization," *International Journal of Impact Engineering*, vol. 32, no. 5, pp. 759–777, 2006.

[9] H. Fang, M. Rais-Rohani, Z. Liu, and M. F. Horstemeyer, "A comparative study of metamodeling methods for multiobjective crashworthiness optimization," *Computers & Structures*, vol. 83, no. 25-26, pp. 2121–2136, 2005.

[10] D. Shangguan, S. Ahuja, and D. M. Stefanescu, "An analytical model for the interaction between an insoluble particle and an advancing solid/liquid interface," *Metallurgical Transactions A*, vol. 23, no. 2, pp. 669–680, 1992.

[11] Y. Zhai, T. H. North, and J. Serrato-Rodrigues, "Transient liquid-phase bonding of alumina and metal matrix composite base materials," *Journal of Materials Science*, vol. 32, no. 6, pp. 1393–1397, 1997.

[12] J. R. Askew, J. F. Wilde, and T. I. Khan, "Transient liquid phase bonding of 2124 aluminium metal matrix composite," *Materials Science and Technology*, vol. 14, no. 9-10, pp. 920–924, 1998.